Aerospace Science and Technology 70 (2017) 396–404

Contents lists available at ScienceDirect

Aerospace Science and Technology

www.elsevier.com/locate/aescte

Review

New approach to study nonlinear dynamic response and vibration of sandwich composite cylindrical panels with auxetic honeycomb core layer

Nguyen Dinh Duc [a,b,c,*], Kim Seung-Eock [c], Ngo Duc Tuan [d], Phuong Tran [d], Nguyen Dinh Khoa [a]

[a] Advanced Materials and Structures Laboratory, VNU-Hanoi – University of Engineering and Technology (UET), 144, Xuan Thuy, Cau Giay, Hanoi, Viet Nam
[b] Infrastructure Engineering Program - VNU-Hanoi, Vietnam–Japan University (VJU), My Dinh 1, Tu Liem, Hanoi, Viet Nam
[c] National Research Laboratory, Department of Civil and Environmental Engineering, Sejong University, 209 Neungdong-ro, Gwangjin-gu, Seoul 05006, Republic of Korea
[d] Department of Infrastructure Engineering, The University of Melbourne, Parkville 3010, VIC, Australia

ARTICLE INFO

Article history:
Received 16 May 2017
Received in revised form 5 August 2017
Accepted 18 August 2017
Available online 24 August 2017

Keywords:
Analytical approach
Nonlinear dynamic response and vibration
Sandwich auxetic composite cylindrical panels
Reddy's first order shear deformation theory
Mechanical, blast and damping loads
Elastic foundations

ABSTRACT

The main goal of this study is using analytical solution to investigate the nonlinear dynamic response and vibration of sandwich auxetic composite cylindrical panels. The sandwich composite panels have three layers in which the top and bottom outer skins are isotropic aluminum materials, the central auxetic core layer – honeycomb structures with negative Poisson's ratio using the same aluminum material. The panels are resting on elastic foundations and subjected to mechanical, blast and damping loads. Based on Reddy's first order shear deformation theory (FSDT) with the geometrical nonlinear in von Karman and using the Airy stress functions method, Galerkin method and fourth-order Runge–Kutta method, the resulting equations are solved to obtain expressions for nonlinear motion equations. The effects of geometrical parameters, material properties, elastic Winkler and Pasternak foundations, mechanical, blast and damping loads on the nonlinear dynamic response and the natural frequencies of sandwich composite cylindrical panels are studied.

© 2017 Elsevier Masson SAS. All rights reserved.

1. Introduction

Most natural materials are characterized by a positive Poisson's ratio, namely they are observed to contract (expand) laterally when stretched (compressed) longitudinally. Nonetheless, the classical theory of elasticity does not preclude the existence of materials with negative Poisson's ratio, known as 'auxetic' after [1]. Auxetic materials are a special and a fascinating material. One example of important applications of auxetic structures in aerospace engineering or in civil engineering is the absorption of powerful impacts such as explosive waves, so they are often used as the outer layer, safeguarding structures inside.

Therefore, recently, auxetic materials have received special attention of a lot of authors in the world. Qiao and Chen [2] studied the impact resistance of uniform and functionally graded auxetic double arrowhead honeycombs, double arrowhead honeycombs (DAHs) are auxetic cellular materials with negative Poisson's ratio (NPR). Grujicic et al. [3] investigated the multi-physics modeling of the fabrication and dynamic performance of all-metal auxetic-hexagonal sandwich-structures. Zhang et al. [4] considered the dynamic thermo-mechanical and impact properties of helical auxetic yarns. Assidi et al. [5] presented the composites with auxetic inclusions showing both an auxetic behavior and enhancement of their mechanical properties. Burlayenko and Sadowski [6] obtained the effective elastic properties of foam-filled honeycomb cores of sandwich panels. Grima et al. [7] investigated the hexagonal honeycombs with zero Poisson's ratios and enhances stiffness. Liu et al. [8] presented the wave propagation in a sandwich plate with a periodic composite core. Wan et al. [9] investigated the study of negative Poisson's ratios in auxetic honeycombs based on a large deflection model. Greaves et al. [10] studied Possion's ratio and modern materials. Zhang et al. [11] investigated the influence of cell micro-structure on the in-plane dynamic crushing of honeycombs with negative Poisson's ratio.

Milton [12] considered the composite materials with Poisson's ratios close to. Tian and Chung [13] studied the wave propagation in sandwich panel with auxetic core. Analytical expressions

* Corresponding author at: Infrastructure Engineering Program - VNU Hanoi, Vietnam–Japan University (VJU), My Dinh 1, Tu Liem, Hanoi, Viet Nam.
E-mail address: ducnd@vnu.edu.vn (N.D. Duc).

http://dx.doi.org/10.1016/j.ast.2017.08.023
1270-9638/© 2017 Elsevier Masson SAS. All rights reserved.

for the dynamic crushing strength of hexagonal honeycombs were derived by Hu and Yu [14]. Strek et al. [15] investigated the finite element analysis of auxetic obstacle deformation and fluid flow in a channel. Strek et al. [16] investigated the effective mechanical properties of concentric cylindrical composites with auxetic phase, the computational analysis of sandwich-structured composites with an auxetic phase [17] and the dynamic response of sandwich panels with auxetic cores [18]. Gabriele Imbalzano et al. [19] studied the three-dimensional modeling of auxetic sandwich panels for localized impact resistance. Thê-Duong Nguyen and Duc [20] considered evaluation of elastic properties and thermal expansion coefficient of composites reinforced by randomly distributed spherical particles with negative Poisson's ratios. Jopek and Strek [21] investigated the thermal and structural dependence of auxetic properties of composite materials. Duc and Cong studied [22] studied the nonlinear dynamic response and vibration of sandwich composite plates with negative Poisson's ratio in auxetic honeycombs. In [23], Duc considered generally and comprehensively about nonlinear static and dynamic stability of FGM plates and shells.

Cylindrical panels play the important part in the modern industries. Therefore, research on static and dynamic response of these structures have received special attention of a lot of authors in the world. Duc et al. [24] investigated the vibration and nonlinear dynamic response of imperfect three-phase polymer nanocomposite panel resting on elastic foundations under hydrodynamic loads. Duc and Quan [25] presented nonlinear buckling and postbuckling of eccentrically stiffened FGM cylindrical panels resting on elastic foundations and subjected to mechanical loads. Duc and Tung [26] proposed the nonlinear response of pressure-loaded functionally graded cylindrical panels with temperature effects. In 2013, Duc [27] also studied the nonlinear dynamic and vibration of eccentrically stiffened FGM double curved shallow shells.

In recent years, the safety of building and structures of infrastructure have become hot issues in all over the world because the negative dynamic loads caused of increasing in terrorist activities, accidental blast. As the results, the composite auxetic material under blast load has gained interests and been studied more. Tan et al. [28] presented the blast-wave impact mitigation using negative effective mass density concept of elastic metamaterials. Adhikary et al. [29] considered the influence of cylindrical charge orientation on the blast response of high strength concrete panels. Zhai et al. [30] investigated the experimental and numerical investigation into RC beams subjected to blast after exposure to fire. Yao et al. [31] presented the experimental and numerical study on the dynamic response of RC slabs under blast loading. Lam et al. [32] studied the response spectrum solutions for blast loading. Imbalzano et al. [33] investigated the auxetic composite panels under blast loadings. Ding and Ngo [34] studied the dynamic response of double skin façades under blast loads. Duc et al. [35] presented the nonlinear dynamic response and vibration of imperfect shear deformable functionally graded plates subjected to blast and thermal loads.

From above literature review [1–17], we can see that there are no studies about dynamic response and vibration of auxetic cylindrical panels yet. Moreover, auxetic plates and shells are complex structures, all published studies on auxetic structures as mentioned above use the Finite element method.

The most significant contribution of this work is using new approach – analytical solution to study nonlinear dynamic response and vibration of sandwich composite panels with negative Poisson's ratio in auxetic honeycombs. This method is more complicated than numerical methods in the aspect of mathematics, especially when using FSTD, but the advantage is that the dynamic response is expressed explicitly through material parameters, geometric parameters of the structure and load, and therefore we can actively control the behavior of the structure by selecting those parameters appropriately.

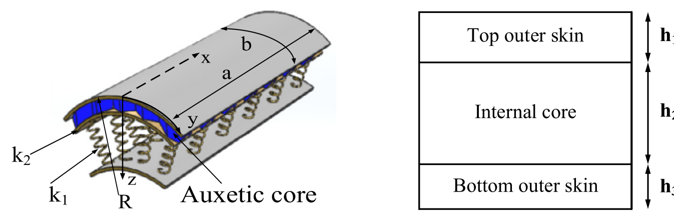

Fig. 1. (left) Model of sandwich composite cylindrical panels on elastic foundations with negative Poisson's ratios in auxetic honeycombs core layer. (right) Dicretization of the sandwich cylindrical panel.

By using analytical approach, this work focuses on studying the nonlinear dynamic response and vibration of the sandwich composite cylindrical panels with negative Poisson's ratio in auxetic honeycombs core structures on elastic foundations subjected to blast and other mechanical loads. The sandwich composite cylindrical panels used in the work have three layers in which the top and bottom outer skins are isotropic aluminum materials, the central core layer has auxetic honeycomb structures using the same aluminum material. The governing equations are derived within the framework of Reddy's first order shear deformation theory, taken into account the von Karman nonlinearity and using the Airy stress function, Galerkin method and fourth-order Runge–Kutta method. The work also analyses and discusses the effects of material and geometrical properties, elastic foundations and mechanical, blast and damping loads on the natural frequency and the nonlinear dynamic response of the composite cylindrical panels.

2. Sandwich composite cylindrical panel with auxetic core layer model

2.1. Model

Consider a sandwich cylindrical panel with auxetic core of radius of curvature R, length of edges a, b and uniform thickness h resting on elastic foundations. A coordinate system (x, y, z) is established, in which the (x, y) plane is in the middle surface of the panel and is z in the thickness direction (Fig. 1, left). The auxetic core which has three layers in which the top and bottom outer skins are isotropic aluminum materials; the central layer has honeycomb structure using the same aluminum material (Fig. 1, right). The bottom outer skin thickness is h_1, internal honeycomb core material thickness is h_2 and top outer skin thickness is h_3, and the total thickness of the shell is $h = h_1 + h_2 + h_3$.

The reaction–deflection relation of Pasternak foundation is given by

$$q_e = k_1 w - k_2 \nabla^2 w \qquad (1)$$

In which $\nabla^2 = \frac{\partial^2}{\partial x^2} + \frac{\partial^2}{\partial y^2}$, w is the deflection of the cylindrical panels, k_1 and k_2 are Winkler foundation modulus and shear layer of Pasternak foundation, respectively.

2.2. Honeycomb core materials

The sandwich composite cylindrical panels having the auxetic honeycomb core layer with negative Poisson's ratio are introduced in this work. Unit cells of core material discussed in the paper are shown in Fig. 2 where l is the length of the inclined cell rib, h is the length of the vertical cell rib, θ is the inclined angle, α and β define the relative cell wall length and the wall's slenderness ratio, respectively, which are important parameters in honeycomb property.

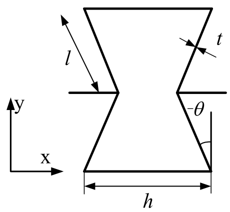

Fig. 2. Geometric of the cell of honeycomb core layer.

Table 1
Poisson's ratio ν_{12} in auxetic honeycomb layer of the composite cylindrical panel at the limit value of small deformation.

	$\frac{h}{l}=1$	$\frac{h}{l}=1.5$	$\frac{h}{l}=2$	$\frac{h}{l}=2.5$	$\frac{h}{l}=3$
$\theta=-35$	−2.7434	−1.2628	−0.8201	−0.6073	−0.4821
$\theta=-45$	−2.4142	−0.8918	−0.5469	−0.3944	−0.3084
$\theta=-50$	−2.3054	−0.7349	−0.4371	−0.3111	−0.2414
$\theta=-60$	−2.1547	−0.4553	−0.3401	−0.1767	−0.1353
$\theta=-75$	−2.0353	−0.1299	−0.0671	−0.0452	−0.0341

Formulas in reference [3] are adopted for calculation of honeycomb core material property

$$\begin{aligned}
&E_1^c = E\left(\frac{t}{l}\right)^3 \frac{\cos\theta}{\left(\frac{h}{l}+\sin\theta\right)\sin^2\theta}, \qquad E_2^c = E\left(\frac{t}{l}\right)^3 \frac{\left(\frac{h}{l}+\sin\theta\right)}{\cos^3\theta}\\
&\nu_{12}^c = \frac{\cos^2\theta}{\left(\frac{h}{l}+\sin\theta\right)\sin\theta}, \qquad G_{12}^c = E\left(\frac{t}{l}\right)^3 \frac{\left(\frac{h}{l}+\sin\theta\right)}{\left(\frac{h}{l}\right)^2\left(1+2\frac{h}{l}\right)\cos\theta}\\
&G_{13}^c = G\frac{t}{l}\frac{\cos\theta}{\frac{h}{l}+\sin\theta}, \qquad G_{23}^c = G\frac{t}{l}\frac{1+2\sin^2\theta}{2\cos\theta\left(\frac{h}{l}+\sin\theta\right)},\\
&\rho_c = \rho\frac{t/l(h/l+2)}{2\cos\theta(h/l+\sin\theta)}
\end{aligned} \tag{2}$$

where symbol "c" represents core material, E, G and ρ are Young's moduli, shear moduli and mass density of the origin material.

To investigate the effect of geometry of the cylindrical panels with negative Poisson's ratio ν_{12} at the limit of small deformation are presented in Table 1 for the combinations of θ and $\frac{h}{l}$. From Table 1, it can be seen that Poisson's ratio ν_{12} increased when geometric parameters of $\frac{h}{l}$ increases and vice versa. The same for in the case geometric parameters of θ decreases, Poisson's ratio ν_{12} increased and vice versa.

3. Theoretical formulations

In this work, Reddy's first order shear deformation theory (FSDT) is used to determine the dynamic response and natural frequency of the panels.

The strain-displacement relations taking into account the von Karman nonlinear terms are [23]

$$\begin{Bmatrix} \varepsilon_x \\ \varepsilon_y \\ \gamma_{yz} \\ \gamma_{xz} \\ \gamma_{xy} \end{Bmatrix} = \begin{Bmatrix} \varepsilon_x^0 \\ \varepsilon_y^0 \\ \gamma_{yz}^0 \\ \gamma_{xz}^0 \\ \gamma_{xy}^0 \end{Bmatrix} + z\begin{Bmatrix} \varepsilon_x^1 \\ \varepsilon_y^1 \\ \gamma_{yz}^1 \\ \gamma_{xz}^1 \\ \gamma_{xy}^1 \end{Bmatrix} = \begin{Bmatrix} \frac{\partial u}{\partial x} + \frac{1}{2}\left(\frac{\partial w}{\partial x}\right)^2 \\ \frac{\partial v}{\partial y} - \frac{w}{R} + \frac{1}{2}\left(\frac{\partial w}{\partial y}\right)^2 \\ \frac{\partial w}{\partial y} + \phi_y \\ \frac{\partial w}{\partial x} + \phi_x \\ \frac{\partial u}{\partial y} + \frac{\partial v}{\partial x} + \frac{\partial w}{\partial x}\frac{\partial w}{\partial y} \end{Bmatrix} + z\begin{Bmatrix} \frac{\partial \phi_x}{\partial x} \\ \frac{\partial \phi_y}{\partial y} \\ 0 \\ 0 \\ \frac{\partial \phi_x}{\partial y} + \frac{\partial \phi_y}{\partial x} \end{Bmatrix} \tag{3}$$

where in the above equations u, v, w are displacement components corresponding to the coordinates (x, y, z), and ϕ_x, ϕ_y are the rotations of normals to the mid-surface with respect to the x and y axes, respectively.

Hooke's law for the sandwich cylindrical panel with negative Poisson's ratio in auxetic honeycomb core layer is defined as follows:

$$\begin{aligned}
&\begin{Bmatrix} \sigma_x^T \\ \sigma_y^T \\ \sigma_{xy}^T \end{Bmatrix} = \begin{bmatrix} Q_{11}^T & Q_{12}^T & 0 \\ Q_{12}^T & Q_{22}^T & 0 \\ 0 & 0 & Q_{66}^T \end{bmatrix} \begin{Bmatrix} \varepsilon_x \\ \varepsilon_y \\ \gamma_{xy} \end{Bmatrix},\\
&\begin{Bmatrix} \sigma_{yz}^T \\ \sigma_{xz}^T \end{Bmatrix} = \begin{bmatrix} Q_{44}^T & 0 \\ 0 & Q_{55}^T \end{bmatrix} \begin{Bmatrix} \gamma_{yz} \\ \gamma_{xz} \end{Bmatrix}\\
&\begin{Bmatrix} \sigma_x^C \\ \sigma_y^C \\ \sigma_{xy}^C \end{Bmatrix} = \begin{bmatrix} Q_{11}^C & Q_{12}^C & 0 \\ Q_{12}^C & Q_{22}^C & 0 \\ 0 & 0 & Q_{66}^C \end{bmatrix} \begin{Bmatrix} \varepsilon_x \\ \varepsilon_y \\ \gamma_{xy} \end{Bmatrix},\\
&\begin{Bmatrix} \sigma_{yz}^C \\ \sigma_{xz}^C \end{Bmatrix} = \begin{bmatrix} Q_{44}^C & 0 \\ 0 & Q_{55}^C \end{bmatrix} \begin{Bmatrix} \gamma_{yz} \\ \gamma_{xz} \end{Bmatrix}\\
&\begin{Bmatrix} \sigma_x^B \\ \sigma_y^B \\ \sigma_{xy}^B \end{Bmatrix} = \begin{bmatrix} Q_{11}^T & Q_{12}^T & 0 \\ Q_{12}^T & Q_{22}^T & 0 \\ 0 & 0 & Q_{66}^T \end{bmatrix} \begin{Bmatrix} \varepsilon_x \\ \varepsilon_y \\ \gamma_{xy} \end{Bmatrix},\\
&\begin{Bmatrix} \sigma_{yz}^B \\ \sigma_{xz}^B \end{Bmatrix} = \begin{bmatrix} Q_{44}^T & 0 \\ 0 & Q_{55}^T \end{bmatrix} \begin{Bmatrix} \gamma_{yz} \\ \gamma_{xz} \end{Bmatrix}
\end{aligned} \tag{4}$$

where above index T, C, B are Top outer skin, Core material, Bottom outer skin respectively.

$$\begin{aligned}
&Q_{11}^C = \frac{E_1^C}{1-\nu_{12}^C\nu_{21}^C}, \qquad Q_{12}^C = \frac{\nu_{12}^C E_2^C}{1-\nu_{12}^C\nu_{21}^C},\\
&Q_{22}^C = \frac{E_2^C}{1-\nu_{12}^C\nu_{21}^C}, \qquad Q_{66}^C = G_{12}^C,\\
&Q_{44}^C = G_{23}^C, \qquad Q_{55}^C = G_{13}^C\\
&Q_{11}^T = Q_{22}^T = \frac{E}{1-\nu^2}, \qquad Q_{12}^T = \frac{\nu E}{1-\nu^2},\\
&Q_{66}^T = Q_{44}^T = Q_{55}^T = \frac{E}{2(1+\nu)}
\end{aligned} \tag{5}$$

The forces and moments of the cylindrical panel can be expressed in terms of stress components across the cylindrical panel thickness as [21,23]:

$$\begin{aligned}
&(N_i, M_i) = \int_{-\frac{h_2}{2}-h_3}^{-\frac{h_2}{2}} \sigma_i^B(1,z)dz + \int_{-\frac{h_2}{2}}^{\frac{h_2}{2}} \sigma_i^C(1,z)dz\\
&\qquad + \int_{\frac{h_2}{2}}^{\frac{h_2}{2}+h_1} \sigma_i^T(1,z)dz, \quad i = x, y, xy\\
&Q_i = K\int_{-\frac{h_2}{2}-h_3}^{-\frac{h_2}{2}} \sigma_{iz}^B dz + K\int_{-\frac{h_2}{2}}^{\frac{h_2}{2}} \sigma_{iz}^C dz + K\int_{\frac{h_2}{2}}^{\frac{h_2}{2}+h_1} \sigma_{iz}^T dz, \quad i = x, y
\end{aligned} \tag{6}$$

Substitution of Eqs. (4) into Eqs. (6) gives the constitutive relations as

$$\begin{Bmatrix} N_x \\ N_y \\ N_{xy} \\ M_x \\ M_y \\ M_{xy} \\ Q_x \\ Q_y \end{Bmatrix} = \begin{bmatrix} A_1 & A_2 & 0 & A_3 & A_4 & 0 & 0 & 0 \\ A_2 & A_5 & 0 & A_4 & A_6 & 0 & 0 & 0 \\ 0 & 0 & A_7 & 0 & 0 & A_8 & 0 & 0 \\ A_3 & A_4 & 0 & A_9 & A_{10} & 0 & 0 & 0 \\ A_4 & A_6 & 0 & A_{10} & A_{11} & 0 & 0 & 0 \\ 0 & 0 & A_8 & 0 & 0 & A_{12} & 0 & 0 \\ 0 & 0 & 0 & 0 & 0 & 0 & KA_{13} & 0 \\ 0 & 0 & 0 & 0 & 0 & 0 & 0 & KA_{15} \end{bmatrix} \times \begin{Bmatrix} \varepsilon_x^0 \\ \varepsilon_y^0 \\ \gamma_{xy}^0 \\ \varepsilon_x^1 \\ \varepsilon_y^1 \\ \gamma_{xy}^1 \\ \gamma_{xz}^0 \\ \gamma_{yz}^0 \end{Bmatrix} \tag{7}$$

where K is the shear correction factors, and $K = \frac{5}{6}$.

$$\begin{aligned}
A_1 &= Q_{11}^C h_2 + Q_{11}^T (h_1 + h_3), \\
A_2 &= Q_{12}^C h_2 + Q_{12}^T (h_1 + h_3), \\
A_3 &= \frac{1}{2} Q_{11}^T \left(h_1 h_2 + h_1^2 - h_2 h_3 - h_3^2\right), \\
A_4 &= \frac{1}{2} Q_{12}^T \left(h_1 h_2 + h_1^2 - h_2 h_3 - h_3^2\right), \\
A_5 &= Q_{22}^C h_2 + Q_{22}^T (h_1 + h_3), \\
A_6 &= \frac{1}{2} Q_{22}^T \left(h_1 h_2 + h_1^2 - h_2 h_3 - h_3^2\right), \\
A_7 &= Q_{66}^C h_2 + Q_{66}^T (h_1 + h_3), \\
A_8 &= \frac{1}{2} Q_{66}^T \left(h_1 h_2 + h_1^2 - h_2 h_3 - h_3^2\right), \\
A_9 &= \frac{1}{12} Q_{11}^C h_2^3 + \frac{1}{3} Q_{11}^T \left[-\frac{h_2^3}{4} + \left(\frac{h_2}{2} + h_3\right)^3 + \left(\frac{h_2}{2} + h_1\right)^3 \right], \\
A_{10} &= \frac{1}{12} Q_{12}^C h_2^3 + \frac{1}{3} Q_{12}^T \left[-\frac{h_2^3}{4} + \left(\frac{h_2}{2} + h_3\right)^3 + \left(\frac{h_2}{2} + h_1\right)^3 \right], \\
A_{11} &= \frac{1}{12} Q_{22}^C h_2^3 + \frac{1}{3} Q_{22}^T \left[-\frac{h_2^3}{4} + \left(\frac{h_2}{2} + h_3\right)^3 + \left(\frac{h_2}{2} + h_1\right)^3 \right], \\
A_{12} &= \frac{1}{12} Q_{66}^C h_2^3 + \frac{1}{3} Q_{66}^T \left[-\frac{h_2^3}{4} + \left(\frac{h_2}{2} + h_3\right)^3 + \left(\frac{h_2}{2} + h_1\right)^3 \right], \\
A_{13} &= Q_{55}^C h_2 + Q_{55}^T (h_1 + h_3), \\
A_{14} &= \frac{1}{2} Q_{55}^T \left(h_1 h_2 + h_1^2 - h_2 h_3 - h_3^2\right), \\
A_{15} &= Q_{44}^C h_2 + Q_{44}^T (h_1 + h_3), \\
A_{16} &= \frac{1}{2} Q_{44}^T \left(h_1 h_2 + h_1^2 - h_2 h_3 - h_3^2\right).
\end{aligned} \tag{8}$$

According to the first-order shear deformation theory, the equations of motion for the cylindrical panels are [23]:

$$\frac{\partial N_x}{\partial x} + \frac{\partial N_{xy}}{\partial y} = I_0 \frac{\partial^2 u}{\partial t^2} + I_1 \frac{\partial^2 \phi_x}{\partial t^2}, \tag{9a}$$

$$\frac{\partial N_{xy}}{\partial x} + \frac{\partial N_y}{\partial y} = I_0 \frac{\partial^2 v}{\partial t^2} + I_1 \frac{\partial^2 \phi_y}{\partial t^2}, \tag{9b}$$

$$\begin{aligned}
&\frac{\partial Q_x}{\partial x} + \frac{\partial Q_y}{\partial y} + N_x \frac{\partial^2 w}{\partial x^2} + 2N_{xy} \frac{\partial^2 w}{\partial x \partial y} + N_y \frac{\partial^2 w}{\partial y^2} + p - k_1 w \\
&\quad + k_2 \left(\frac{\partial^2 w}{\partial x^2} + \frac{\partial^2 w}{\partial y^2} \right) + \frac{N_y}{R} = I_0 \frac{\partial^2 w}{\partial t^2} + 2\varepsilon I_0 \frac{\partial w}{\partial t}
\end{aligned} \tag{9c}$$

$$\frac{\partial M_x}{\partial x} + \frac{\partial M_{xy}}{\partial y} - Q_x = I_2 \frac{\partial^2 \phi_x}{\partial t^2} + I_1 \frac{\partial^2 u}{\partial t^2}, \tag{9d}$$

$$\frac{\partial M_{xy}}{\partial x} + \frac{\partial M_y}{\partial y} - Q_y = I_2 \frac{\partial^2 \phi_y}{\partial t^2} + I_1 \frac{\partial^2 v}{\partial t^2}, \tag{9e}$$

where ε is the damping coefficient [24], and

$$I_i = \int_{-\frac{h_2}{2}-h_3}^{-\frac{h_2}{2}} \rho^B z^i dz + \int_{-\frac{h_2}{2}}^{\frac{h_2}{2}} \rho^C z^i dz + \int_{\frac{h_2}{2}}^{\frac{h_2}{2}+h_1} \rho^T z^i dz \quad (i = 0, 1, 2) \tag{10}$$

The blast load $p(t)$ is a short-term load and generated by an explosion or by a shock-wave disturbance produced by an aircraft flying at supersonic speed, or by a supersonic projectile, rocket or missile operating in its vicinity. It can be expressed as [32–35]

$$p(t) = 1.8 Ps_{max} \left(1 - \frac{t}{T_s}\right) \exp\left(\frac{-bt}{T_s}\right), \tag{11}$$

where the "1.8" factor accounts for the effects of a hemispherical blast, Ps_{max} is the maximum (or peak) static over-pressure, b is the parameter controlling the rate of wave amplitude decay and T_s is the parameter characterizing the duration of the blast pulse.

From the constitutive relations in Eq. (7), one can write

$$\begin{aligned}
\varepsilon_x^0 &= -\frac{A_5}{A_2^2 - A_1 A_5} N_x + \frac{A_2}{A_2^2 - A_1 A_5} N_y + \frac{A_3 A_5 - A_2 A_4}{A_2^2 - A_1 A_5} \varepsilon_x^1 \\
&\quad + \frac{A_4 A_5 - A_2 A_6}{A_2^2 - A_1 A_5} \varepsilon_y^1, \\
\varepsilon_y^0 &= \frac{A_2}{A_2^2 - A_1 A_5} N_x - \frac{A_1}{A_2^2 - A_1 A_5} N_y + \frac{A_1 A_4 - A_2 A_3}{A_2^2 - A_1 A_5} \varepsilon_x^1 \\
&\quad + \frac{A_1 A_6 - A_2 A_4}{A_2^2 - A_1 A_5} \varepsilon_y^1 \\
\gamma_{xy}^0 &= \frac{1}{A_7} N_{xy} - \frac{A_8}{A_7} \gamma_{xy}^1
\end{aligned} \tag{12}$$

The stress function $f(x, y, t)$ is introduced as

$$N_x = \frac{\partial^2 f}{\partial y^2}, \qquad N_y = \frac{\partial^2 f}{\partial x^2}, \qquad N_{xy} = -\frac{\partial^2 f}{\partial x \partial y}. \tag{13}$$

Replacing Eq. (13) into Eqs. (9a) and (9b) gives

$$\frac{\partial^2 u}{\partial t^2} = -\frac{I_1}{I_0} \frac{\partial^2 \phi_x}{\partial t^2}, \tag{14a}$$

$$\frac{\partial^2 v}{\partial t^2} = -\frac{I_1}{I_0} \frac{\partial^2 \phi_y}{\partial t^2}. \tag{14b}$$

Substituting Eqs. (14a) and (14b) into Eqs. (9c)–(9e) yields

$$\begin{aligned}
&\frac{\partial Q_x}{\partial x} + \frac{\partial Q_y}{\partial y} + \frac{\partial^2 f}{\partial y^2} \frac{\partial^2 w}{\partial x^2} - 2 \frac{\partial^2 f}{\partial x \partial y} \frac{\partial^2 w}{\partial x \partial y} + \frac{\partial^2 f}{\partial x^2} \frac{\partial^2 w}{\partial y^2} \\
&\quad + p - k_1 w + k_2 \left(\frac{\partial^2 w}{\partial x^2} + \frac{\partial^2 w}{\partial y^2} \right) \\
&\quad + \frac{1}{R} \frac{\partial^2 f}{\partial x^2} = I_0 \frac{\partial^2 w}{\partial t^2} + 2\varepsilon I_0 \frac{\partial w}{\partial t},
\end{aligned} \tag{15a}$$

$$\frac{\partial M_x}{\partial x}+\frac{\partial M_{xy}}{\partial y}-Q_x=\left(I_2-\frac{I_1^2}{I_0}\right)\frac{\partial^2\phi_x}{\partial t^2}, \tag{15b}$$

$$\frac{\partial M_{xy}}{\partial x}+\frac{\partial M_y}{\partial y}-Q_y=\left(I_2-\frac{I_1^2}{I_0}\right)\frac{\partial^2\phi_y}{\partial t^2}. \tag{15c}$$

By substituting Eqs. (12) into Eqs. (7) and then into Eqs. (15), the system of motion Eqs. (15) is rewritten as follows

$$H_{11}(w)+H_{12}(\phi_x)+H_{13}(\phi_y)+S(w,f)+p = I_o\frac{\partial^2 w}{\partial t^2}+2\varepsilon I_0\frac{\partial w}{\partial t}, \tag{16a}$$

$$H_{21}(w)+H_{22}(\phi_x)+H_{23}(\phi_y)+H_{24}(f) = \left(I_2-\frac{I_1^2}{I_0}\right)\frac{\partial^2\phi_x}{\partial t^2}, \tag{16b}$$

$$H_{31}(w)+H_{32}(\phi_x)+H_{33}(\phi_y)+H_{34}(f) = \left(I_2-\frac{I_1^2}{I_o}\right)\frac{\partial^2\phi_y}{\partial t^2}, \tag{16c}$$

where

$$H_{11}(w)=KA_{13}\frac{\partial^2 w}{\partial x^2}+KA_{15}\frac{\partial^2 w}{\partial y^2}-k_1 w+k_2\left(\frac{\partial^2 w}{\partial x^2}+\frac{\partial^2 w}{\partial y^2}\right),$$

$$H_{12}(\phi_x)=KA_{13}\frac{\partial\phi_x}{\partial x},\qquad H_{13}(\phi_y)=KA_{15}\frac{\partial\phi_y}{\partial y},$$

$$S(w,f)=\frac{\partial^2 f}{\partial y^2}\frac{\partial^2 w}{\partial x^2}-2\frac{\partial^2 f}{\partial x\partial y}\frac{\partial^2 w}{\partial x\partial y}+\frac{\partial^2 f}{\partial x^2}\frac{\partial^2 w}{\partial y^2}+\frac{1}{R}\frac{\partial^2 f}{\partial x^2},$$

$$H_{21}(w)=-KA_{13}\frac{\partial w}{\partial x},$$

$$H_{22}(\phi_x)=D_{11}\frac{\partial^2\phi_x}{\partial x^2}+D_{66}\frac{\partial^2\phi_x}{\partial y^2}-KA_{13}\phi_x,$$

$$H_{23}(\phi_y)=(D_{12}+D_{66})\frac{\partial^2\phi_y}{\partial x\partial y},$$

$$H_{24}(f)=\left(\frac{A_2A_4-A_3A_5}{A_2^2-A_1A_5}-\frac{A_8}{A_7}\right)\frac{\partial^3 f}{\partial x\partial y^2}+\frac{A_2A_3-A_1A_4}{A_2^2-A_1A_5}\frac{\partial^3 f}{\partial x^3},$$

$$H_{31}(w)=-KA_{15}\frac{\partial w}{\partial y},\qquad H_{32}(\phi_x)=(D_{21}+D_{66})\frac{\partial^2\phi_x}{\partial x\partial y},$$

$$H_{33}(\phi_y)=(D_{22})\frac{\partial^2\phi_y}{\partial y^2}+(D_{66})\frac{\partial^2\phi_y}{\partial x^2}-KA_{15}\phi_y,$$

$$H_{34}(f)=\left(\frac{A_2A_4-A_1A_6}{A_2^2-A_1A_5}-\frac{A_8}{A_7}\right)\frac{\partial^3 f}{\partial x^2\partial y}+\frac{A_2A_6-A_4A_5}{A_2^2-A_1A_5}\frac{\partial^3 f}{\partial y^3},$$

$$D_{11}=\frac{A_3^2A_5-2A_2A_3A_4+A_1A_4^2}{A_2^2-A_1A_5}+A_9,$$

$$D_{66}=A_{12}-\frac{A_8^2}{A_7},$$

$$D_{12}=\frac{A_3(A_4A_5-A_2A_6)+A_4(A_1A_6-A_2A_4)}{A_2^2-A_1A_5}+A_{10},$$

$$D_{21}=\frac{A_4(A_3A_5-A_2A_4)+A_6(A_1A_4-A_2A_3)}{A_2^2-A_1A_5}+A_{10},$$

$$D_{22}=\frac{A_4^2A_5-2A_2A_4A_6+A_1A_6^2}{A_2^2-A_1A_5}+A_{11}.$$

The geometric compatibility equation for a cylindrical panel is written as [6,23]

$$\frac{\partial^2\varepsilon_x^0}{\partial y^2}+\frac{\partial^2\varepsilon_y^0}{\partial x^2}-\frac{\partial^2\gamma_{xy}^0}{\partial x\partial y}=\left(\frac{\partial^2 w}{\partial x\partial y}\right)^2-\frac{\partial^2 w}{\partial x^2}\frac{\partial^2 w}{\partial y^2}-\frac{1}{R}\frac{\partial^2 w}{\partial x^2}. \tag{17}$$

Set Eqs. (13) and (12) into the deformation compatibility equation (17), we obtain

$$\begin{aligned}&-\frac{A_1}{A_2^2-A_1A_5}\frac{\partial^4 f}{\partial x^4}-\frac{A_5}{A_2^2-A_1A_5}\frac{\partial^4 f}{\partial y^4}\\&+\left(\frac{2A_2}{A_2^2-A_1A_5}+\frac{1}{A_7}\right)\frac{\partial^4 f}{\partial x^2\partial y^2}\\&+\left(\frac{A_3A_5-A_2A_4}{A_2^2-A_1A_5}+\frac{A_8}{A_7}\right)\frac{\partial^3\phi_x}{\partial x\partial y^2}+\frac{A_1A_4-A_2A_3}{A_2^2-A_1A_5}\frac{\partial^3\phi_x}{\partial x^3}\\&+\frac{A_4A_5-A_2A_6}{A_2^2-A_1A_5}\frac{\partial^3\phi_y}{\partial y^3}+\left(\frac{A_1A_6-A_2A_4}{A_2^2-A_1A_5}+\frac{A_8}{A_7}\right)\frac{\partial^3\phi_y}{\partial x^2\partial y}\\&=\left(\frac{\partial^2 w}{\partial x\partial y}\right)^2-\frac{\partial^2 w}{\partial x^2}\frac{\partial^2 w}{\partial y^2}-\frac{1}{R}\frac{\partial^2 w}{\partial x^2}.\end{aligned} \tag{18}$$

Eqs. (16) and (18) are nonlinear equations in terms of variables w,ϕ_x,ϕ_y and f and are used to investigate the nonlinear vibration and dynamic stability of the cylindrical panels with negative Poisson's ratio in auxetic honeycombs using the first order shear deformation theory.

Considering the following boundary condition [5], four edges of cylindrical panel are simply supported; immovable edges is under blast load p. Thus, the boundary conditions are

$$\begin{aligned}&w=N_{xy}=\phi_y=M_x=0,\qquad N_x=-P_xh \text{ at } x=0,a,\\&w=N_{xy}=\phi_x=M_y=0,\qquad N_y=-P_yh \text{ at } y=0,b.\end{aligned} \tag{19}$$

The mentioned conditions in (19) can be satisfied identically if the approximate solutions are represented by:

$$\begin{aligned}&w(x,y,t)=W(t)\sin\lambda_m x\sin\delta_n y,\\&\phi_x(x,y,t)=\Phi_x(t)\cos\lambda_m x\sin\delta_n y,\\&\phi_y(x,y,t)=\Phi_y(t)\sin\lambda_m x\cos\delta_n y,\end{aligned} \tag{20}$$

$$f(x,y,t)=B_1\cos 2\lambda_m x+B_2\cos 2\delta_n y+B_3\sin\lambda_m x\sin\delta_n y -\frac{1}{2}P_xhy^2-\frac{1}{2}P_yhx^2, \tag{21}$$

where $\lambda_m=\frac{m\pi}{a}$, $\delta_n=\frac{n\pi}{b}$, $m,n=1,2,\ldots$ are the natural numbers of half waves in the corresponding direction x, y, and W,Φ_x,Φ_y – the amplitudes which are functions dependent on time.

$$B_1=\frac{A_1A_5-A_2^2}{32A_1}\frac{\delta_n^2}{\lambda_m^2}W^2(t),\qquad B_2=\frac{A_1A_5-A_2^2}{32A_5}\frac{\lambda_m^2}{\delta_n^2}W^2(t),$$
$$B_3=a_1W^2(t)+a_2\Phi_x(t)+a_3\Phi_y(t), \tag{22}$$

where

$$a_1=\frac{\lambda_m^2}{R\left[\frac{A_1}{A_2^2-A_1A_5}\lambda_m^4+\frac{A_5}{A_2^2-A_1A_5}\delta_n^4-\left(\frac{2A_2}{A_2^2-A_1A_5}+\frac{1}{A_7}\right)\lambda_m^2\delta_n^2\right]}$$

$$a_2=\frac{\left[\left(\frac{A_3A_5-A_2A_4}{A_2^2-A_1A_5}+\frac{A_8}{A_7}\right)\lambda_m\delta_n^2+\frac{A_1A_4-A_2A_3}{A_2^2-A_1A_5}\lambda_m^3\right]}{\frac{A_1}{A_2^2-A_1A_5}\lambda_m^4+\frac{A_5}{A_2^2-A_1A_5}\delta_n^4-\left(\frac{2A_2}{A_2^2-A_1A_5}+\frac{1}{A_7}\right)\lambda_m^2\delta_n^2}$$

$$a_3=\frac{\left[\frac{A_4A_5-A_2A_6}{A_2^2-A_1A_5}\delta_n^3+\left(\frac{A_1A_6-A_2A_4}{A_2^2-A_1A_5}+\frac{A_8}{A_7}\right)\lambda_m^2\delta_n\right]}{\frac{A_1}{A_2^2-A_1A_5}\lambda_m^4+\frac{A_5}{A_2^2-A_1A_5}\delta_n^4-\left(\frac{2A_2}{A_2^2-A_1A_5}+\frac{1}{A_7}\right)\lambda_m^2\delta_n^2}.$$

Replacing Eqs. (19)–(21) into Eqs. (16), and then applying the Galerkin method to the resulting equations yields:

$$h_{11}W+h_{12}\Phi_x+h_{13}\Phi_y+h_{14}\Phi_xW+h_{15}\Phi_yW+h_{16}W^2 +h_{17}W^3+h_{18}+p\frac{4}{\lambda_m\delta_n}=\frac{ab}{4}\left(I_o\frac{\partial^2 w}{\partial t^2}+2\varepsilon I_o\frac{\partial w}{\partial t}\right), \tag{23a}$$

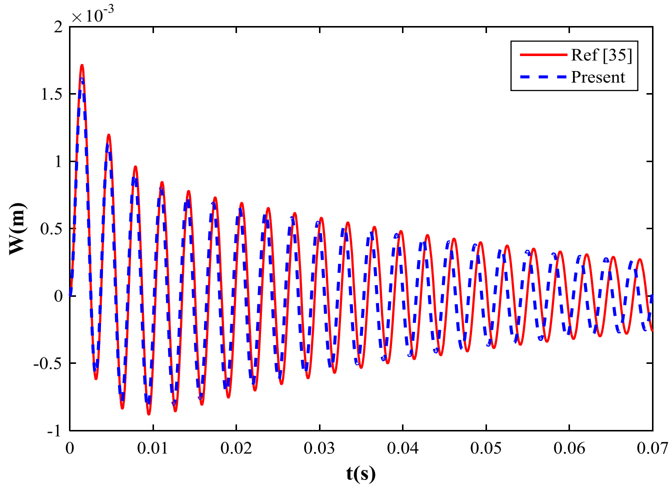

Fig. 3. Comparison of nonlinear dynamic response of plate on elastic foundations subjected to blast load with results in [35].

$$h_{21}W + h_{22}\Phi_x + h_{23}\Phi_y + h_{24}W^2 = \rho_1\frac{\partial^2\phi_x}{\partial t^2} \tag{23b}$$

$$h_{31}W + h_{32}\Phi_x + h_{33}\Phi_y + h_{34}W^2 = \rho_1\frac{\partial^2\phi_y}{\partial t^2} \tag{23c}$$

in which the detail of coefficients $h_{1i}(i=\overline{1,8})$, $h_{jk}(j=\overline{2,3}, k=\overline{1,4})$, ρ_1 may be found in Appendix.

Taking linear parts of the set of Eqs. (23), the natural frequencies of the shell can be determined directly by solving determinant

$$\begin{vmatrix} h_{11}+I_0\omega^2 & h_{12} & h_{13} \\ h_{21} & h_{22}+\rho_1\omega^2 & h_{23} \\ h_{31} & h_{32} & h_{33}+\rho_1\omega^2 \end{vmatrix} = 0 \tag{24}$$

Solving Eqs. (24) yields three angular frequencies, the smallest one is being considered.

4. Numerical results and discussion

The parameters for the geometric parameters of sandwich cylindrical panels with negative Poisson's ratio in core layer were chosen as below:

$$m=n=1,\quad b/a=1,\quad b/h=20,\quad h/l=2,$$
$$t/l=0.0138751,\quad b/R=1/2,\quad \theta=-50^\circ,$$
$$E=68.2\text{ GPa},\quad \nu=0.33,\quad \rho=2700\text{ kg/m}^3,$$
$$G=26\text{ GPa}\quad h_1=h_3=0.00667\text{ m},\quad h_2=0.02.$$

4.1. Numerical verification

To evaluate the reliability of the method used in the paper, we have compared our results with the findings in Ref. [35]. If we chose $R\to\infty$, the nonlinear dynamic response of panel cylindrical will turn into the nonlinear dynamic response of plate. Fig. 3 shows the comparison between present of the nonlinear dynamic response of plate with only made of ceramic ($N=0$) on the elastic foundations subjected to blast load and the result of Duc et al in [35]. In this work, the authors considered the nonlinear dynamic and vibration of FGM plates subjected to blast loads with the volume fraction index $N=0$. From Fig. 3, it can be seen that a good agreement is obtained in this comparison.

The geometry parameters and material parameters in Fig. 3 are chosen as follows [22]

Table 2
Effect of elastic foundation and mechanical load on natural frequencies $\omega(1/s)$ of the cylindrical panels with auxetic core layer ($\nu_{12}=-0.4371$).

	$k_2=0$	$k_2=0.02$ GPa m	$k_2=0.04$ GPa m
$P_x=0$			
$k_1=0$	7259	8717	9964
$k_1=0.3$ GPa/m	7782	9157	10351
$k_1=0.5$ GPa/m	8112	9439	10602
$P_x=0.3$ GPa			
$k_1=0$	6846	8376	9667
$k_1=0.3$ GPa/m	7398	8834	10066
$k_1=0.5$ GPa/m	7745	9126	10323
$P_x=0.5$ GPa			
$k_1=0$	6557	8141	9464
$k_1=0.3$ GPa/m	7131	8611	9871
$k_1=0.5$ GPa/m	7490	8910	10134

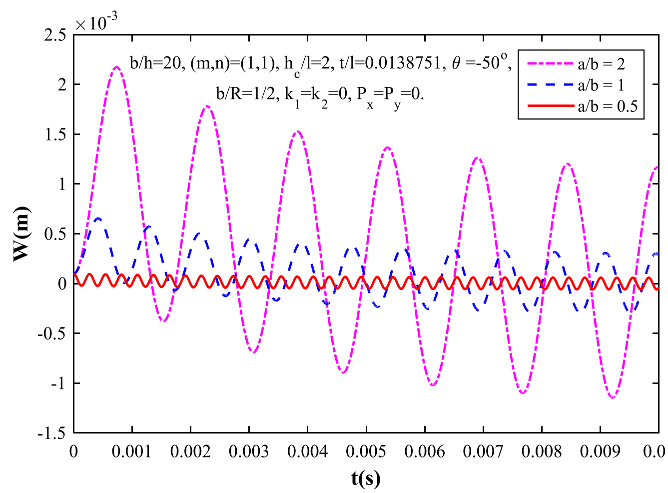

Fig. 4. Effects of ratio a/b on the nonlinear dynamic response of the cylindrical panels with negative Poisson's ratio in core layer under blast load.

$$N=0,\quad m=n=1,\quad b/a=1,\quad b/h=20,$$
$$k_1=0.3\text{ GPa/m},\quad k_2=0.02\text{ GPa m},\quad T=(300+350)\text{ K}$$
$$E_1^c=E_2^c=E=384.43\times10^9(0\times T^{-1}+1-3.07\times10^{-4}T$$
$$+2.16\times10^{-7}T^2-8.94\times10^{-11}T^3)\text{ Pa},$$
$$G_{12}^c=G_{13}^c=G_{23}^c=G=\frac{E}{2(1+\nu)},$$
$$\rho=\rho_c=2370\text{ kg/m}^3.$$

4.2. Nonlinear dynamic response

The effect of elastic foundations and pre-loaded axial on the natural frequency of the cylindrical panel with auxetic core are shown in Table 2 ($\nu_{12}=-0.4371$). The value of the natural frequency increases when the values k_1 and k_2 increase and the natural frequency decreases when the value P_x increases. It can be seen that elastic foundations have positive effect whilst P_x has negative effect on the natural frequency value. Furthermore, the Pasternak elastic foundation influences on the natural frequency larger than the Winkler foundation.

Fig. 4 shows the influence of ratio $a/b=(0.5,1,2)$ on the nonlinear dynamic response of the sandwich cylindrical panels ($\nu_{12}=-0.4371$) under blast loads. From Fig. 4, it can be seen that when a/b is increased, the value of the panels amplitude increases and vice versa.

Fig. 5 shows the effects of ratio $b/h=(20,30,40)$ on the nonlinear dynamic response of the sandwich cylindrical panels ($\nu_{12}=-0.4371$) under blast loads. It is obvious that, the higher the ratio b/h, the higher the amplitude of the panels.

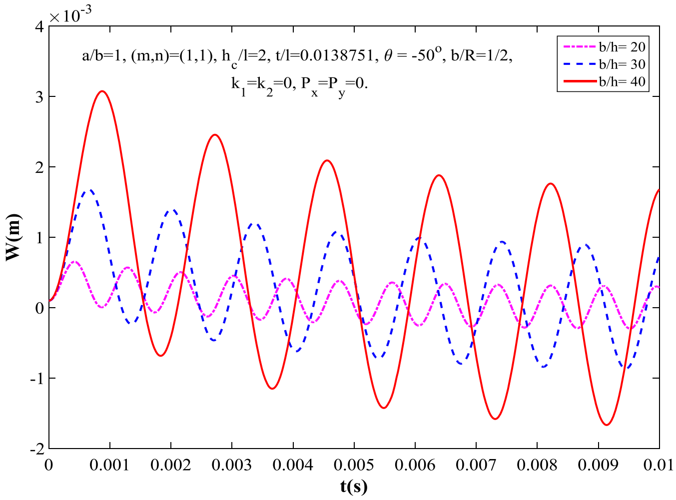

Fig. 5. Effects of ratio a/b on the nonlinear dynamic response of the cylindrical panels with negative Poisson's ratio in core layer under blast load.

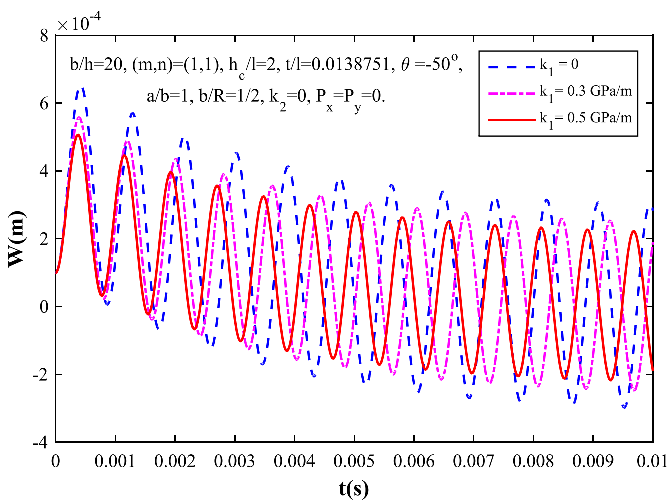

Fig. 6. Effect of the linear Winkler foundation on the nonlinear dynamic response of the sandwich composite cylindrical panels.

Figs. 6 and 7 consider the effects of coefficients k_1, k_2 of the linear Winkler and Pasternak foundations, respectively, on the nonlinear dynamic response of the sandwich panels under blast loads. From the figures, we can see that the amplitude fluctuation of the panels with negative Poisson's ratio ($\nu_{12} = -0.4371$) decreases when the coefficients of elastic foundations increase. In addition, compared with the case of corresponding to the coefficient k_1 of the Winkler model, the Pasternak type elastic foundation with coefficient k_2 has a stronger effect.

Fig. 8 illustrates the effect of parameter characterizing the duration of the blast pulse on nonlinear response of the cylindrical panels for three cases $T_s = (0.005, 0.01, 0.02)$. From this figure, as our expectation, the amplitude of vibration increases with increase in the value of the parameter characterizing the duration of the blast pulse T_s and vice versa.

Fig. 9 shows the variation of nonlinear dynamic response amplitudes of the sandwich panels ($\nu_{12} = -0.4371$) with various values of pre-loaded axial compression P_x. It can be seen that the amplitude fluctuation of the panels increases when the value of pre-loaded axial compression force P_x increases.

Fig. 10 illustrates the effect of damping on amplitude–time curves for nonlinear dynamic response of the sandwich panels with three values of damping coefficient $\varepsilon = (0.1, 5, 8)$. From

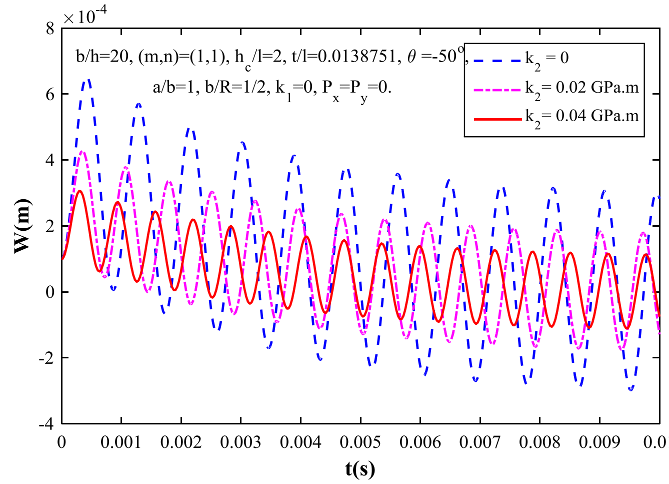

Fig. 7. Effect of the Pasternak foundation on the nonlinear dynamic response of the sandwich composite cylindrical panels.

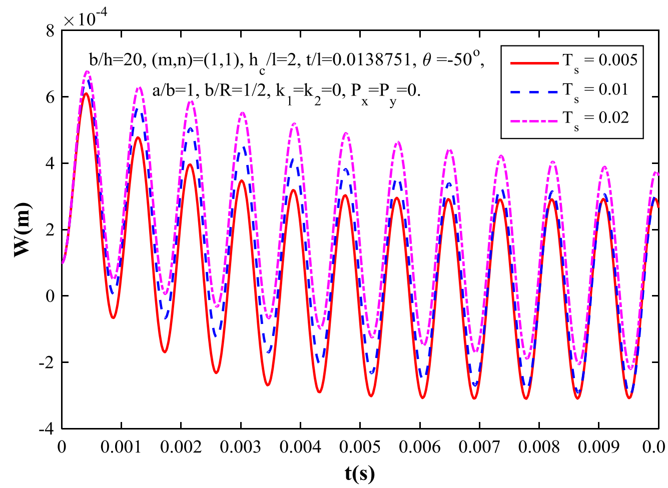

Fig. 8. Effect of parameter characterizing the duration of the blast pulse T_s on nonlinear response of the sandwich composite cylindrical panels.

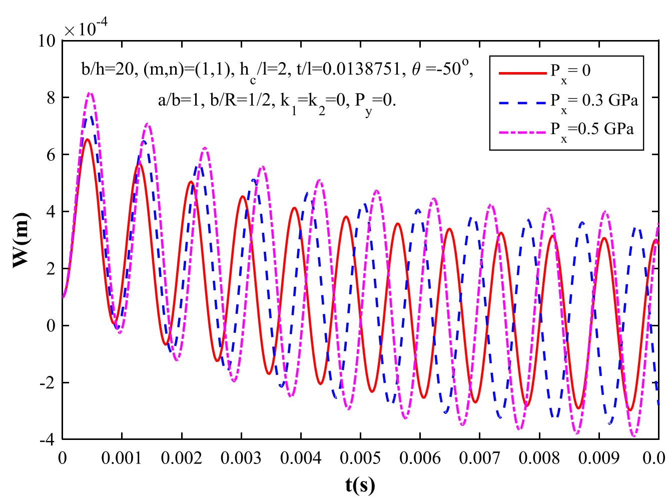

Fig. 9. Effect of pre-loaded axial P_x compression on nonlinear response of the sandwich composite cylindrical panels.

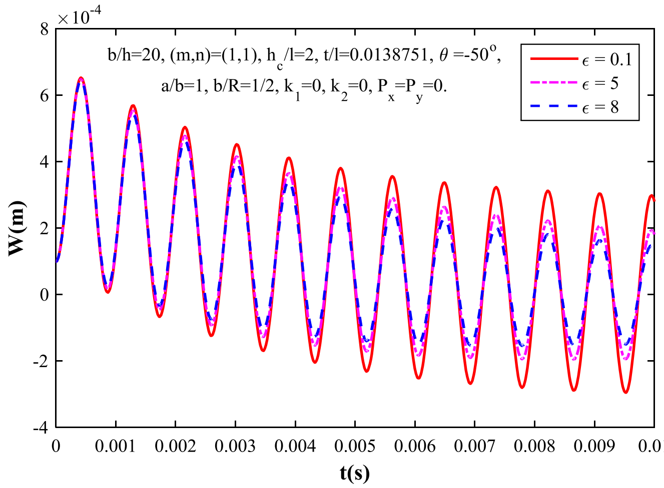

Fig. 10. Effect of damping coefficient ε on the nonlinear dynamic response of the sandwich composite panels under blast loads.

Fig. 10, it can be observed that the damping influences on the nonlinear response of the shell are very small in the first vibration periods.

5. Conclusion

Auxetic material with negative Poisson's ratio is a special and fascinating material. In this work, using analytical approach, the nonlinear dynamic response and vibration of the sandwich composite cylindrical panels on elastic foundations with negative Poisson's ratio core layer under mechanical, blast and damping loads are studied. Reddy's first order shear deformation theory, the Airy stress function and Galerkin method are used to form the basic equations to determine the dynamic response and the natural frequencies of the composite panels. The numerical results are investigated by the Runge–Kutta procedure.

The work has analyzed and discussed the effects of material and geometrical properties, elastic foundations, mechanical, blats and damping loads on the natural frequencies and the nonlinear dynamic response of the sandwich composite panels. Our most important finding by analytical solution is the dynamic response and natural frequency could be explicitly represented in these input parameters. As the result, we are able to design a suitable auxetic composite structures under the blast and other mechanical loads.

A point to be emphasized is that within the framework of this work, we only consider a certain case in which the middle core layer is an auxetic layer (having cell structure as shown in Fig. 2). When the middle layer consists of a number of auxetic layers that are connected together in the form of a honeycomb, the effect of reducing shocks will be stronger [29–34]. However, in that case, it is important to know exactly how many independent elastic modulus the honeycomb structure has, how strain-displacement relation is so that we can apply the analytical solutions. Unfortunately, until now, there have been no experimental and theoretical publishments covering all mechanical–physical parameters of this multi-layered structures.

Funding

This research is funded by Vietnam National Foundation for Science and Technology Development (NAFOSTED) under grant number 107.02-2015.03. The authors are grateful for this support.

Conflict of interest statement

The authors declare no conflict of interest.

Appendix

$$h_{11} = -KA_{13}\lambda_m^2\frac{ab}{4} - KA_{15}\delta_n^2\frac{ab}{4} - k_1\frac{ab}{4} - k_2\left(\lambda_m^2+\delta_n^2\right)\frac{ab}{4} + P_x h\lambda_m^2\frac{ab}{4} + P_y h\delta_n^2\frac{ab}{4},$$

$$h_{12} = -KA_{13}\lambda_m\frac{ab}{4} - \frac{\lambda_m^2}{R}\frac{ab}{4}a_2,$$

$$h_{13} = -KA_{15}\delta_n\frac{ab}{4} - \frac{\lambda_m^2}{R}\frac{ab}{4}a_3, \qquad h_{14} = \frac{8}{3}a_2\lambda_m^3\delta_n^3,$$

$$h_{15} = a_3\frac{8}{3}\lambda_m^3\delta_n^3,$$

$$h_{16} = \frac{1}{6}\frac{A_1A_5-A_2^2}{A_1}\frac{\delta_n}{\lambda_m} - \frac{\lambda_m^2}{R}\frac{ab}{4}a_1,$$

$$h_{17} = -\frac{A_1A_5-A_2^2}{64A_5}ab\lambda_m^4 + \frac{8}{3}a_1\lambda_m^3\delta_n^3 - \frac{A_1A_5-A_2^2}{64A_1}ab\delta_n^4,$$

$$h_{18} = -\frac{4}{\lambda_m\delta_n}\frac{P_y h}{R}, \qquad h_{21} = -KA_{13}\lambda_m\frac{ab}{4},$$

$$h_{22} = -(D_{11})\lambda_m^2\frac{ab}{4} - (D_{66})\delta_n^2\frac{ab}{4} - KA_{13}\frac{ab}{4} - \left(\left(\frac{A_2A_4-A_3A_5}{A_2^2-A_1A_5} - \frac{A_8}{A_7}\right)\lambda_m\delta_n^2 + \frac{A_2A_3-A_1A_4}{A_2^2-A_1A_5}\lambda_m^3\right)\frac{ab}{4}a_2$$

$$h_{23} = -(D_{12}+D_{66})\lambda_m\delta_n\frac{ab}{4} - \left(\left(\frac{A_2A_4-A_3A_5}{A_2^2-A_1A_5} - \frac{A_8}{A_7}\right)\lambda_m\delta_n^2 + \frac{A_2A_3-A_1A_4}{A_2^2-A_1A_5}\lambda_m^3\right)\frac{ab}{4}a_3,$$

$$h_{24} = \frac{2}{3}\frac{A_2A_3-A_1A_4}{A_2^2-A_1A_5}\frac{A_1A_5-A_2^2}{A_1}\delta_n - \left(\left(\frac{A_2A_4-A_3A_5}{A_2^2-A_1A_5} - \frac{A_8}{A_7}\right)\lambda_m\delta_n^2 + \frac{A_2A_3-A_1A_4}{A_2^2-A_1A_5}\lambda_m^3\right)\frac{ab}{4}a_1,$$

$$h_{31} = -KA_{15}\delta_n\frac{ab}{4},$$

$$h_{32} = -(D_{21}+D_{66})\lambda_m\delta_n\frac{ab}{4} - \left[\left(\frac{A_2A_4-A_1A_6}{A_2^2-A_1A_5} - \frac{A_8}{A_7}\right)\lambda_m^2\delta_n + \frac{A_2A_6-A_4A_5}{A_2^2-A_1A_5}\delta_n^3\right]\frac{ab}{4}a_2,$$

$$h_{33} = -(D_{22})\frac{ab}{4}\delta_n^2 - (D_{66})\frac{ab}{4}\lambda_m^2 - KA_{15}\frac{ab}{4} - \left[\left(\frac{A_2A_4-A_1A_6}{A_2^2-A_1A_5} - \frac{A_8}{A_7}\right)\lambda_m^2\delta_n + \frac{A_2A_6-A_4A_5}{A_2^2-A_1A_5}\delta_n^3\right]\frac{ab}{4}a_3,$$

$$h_{34} = \frac{2}{3}\frac{A_2A_6 - A_4A_5}{A_2^2 - A_1A_5}\frac{A_1A_5 - A_2^2}{A_5}\lambda_m - \left[\left(\frac{A_2A_4 - A_1A_6}{A_2^2 - A_1A_5} - \frac{A_8}{A_7}\right)\lambda_m^2\delta_n\rho_1 = \left(I_2 - \frac{I_1^2}{I_0}\right)\frac{ab}{4}. + \frac{A_2A_6 - A_4A_5}{A_2^2 - A_1A_5}\delta_n^3\right]\frac{ab}{4}a_1,$$

References

[1] K.E. Evans, M.A. Nkansah, I.J. Hutchinson, et al., Molecular network design, Nature 353 (1991) 124.

[2] J.X. Qiao, C.Q. Chen, Impact resistance of uniform and functionally graded auxetic double arrowhead honeycombs, Int. J. Impact Eng. 83 (2015) 47–58.

[3] M. Grujicic, R. Galgalikar, J.S. Snipes, et al., Multi-physics modeling of the fabrication and dynamic performance of all-metal auxetic-hexagonal sandwich-structures, Mater. Des. 51 (2013) 113–130.

[4] G. Zhang, O.R. Ghita, K. Evans, Dynamic thermo-mechanical and impact properties of helical auxetic yarns, Composites, Part B, Eng. 99 (2016) 494–505.

[5] M. Assidi, J. Ganghoffer, Composites with auxetic inclusions showing both an auxetic behavior and enhancement of their mechanical properties, Compos. Struct. 94 (2012) 2373–2382.

[6] V.N. Burlayenko, T. Sadowski, Effective elastic properties of foam-filled honeycomb cores of sandwich panels, Compos. Struct. 92 (2010) 2890–2900.

[7] J.N. Grima, L. Oliveri, D. Attard, et al., Hexagonal honeycombs with zero Poisson's ratios and enhances stiffness, Adv. Eng. Mater. 12 (9) (2010) 855–862.

[8] X.F. Liu, Y.F. Wang, Y.S. Wang, et al., Wave propagation in a sandwich plate with a periodic composite core, J. Sandw. Struct. Mater. 16 (3) (2014) 319–338.

[9] H. Wan, H. Ohtaki, S. Kotosaka, et al., A study of negative Poisson's ratios in auxetic honeycombs based on a large deflection model, Eur. J. Mech. 23 (2014) 95–106.

[10] G.N. Greaves, A.L. Greer, R.S. Lakes, et al., Possion's ratio and modern materials, Nat. Mater. 10 (2011) 823–837.

[11] X.C. Zhang, L.Q. An, H.M. Ding, et al., The influence of cell micro-structure on the inplane dynamic crushing of honeycombs with negative Poisson's ratio, J. Sandw. Struct. Mater. 17 (1) (2015) 26–55.

[12] G.W. Milton, Composite materials with Poisson's ratios close to −1, J. Mech. Phys. Solids 40 (1992) 1105–1137.

[13] D.Q. Tian, Y.Z. Chun, Wave propagation in sandwich panel with auxetic core, J. Solids Mech. 2 (2010) 393–402.

[14] L.L. Hu, T.X. Yu, Dynamic crushing strength of hexagonal honeycombs, Int. J. Impact Eng. 37 (2010) 467–474.

[15] T. Strek, P. Kedziora, B. Maruszewski, et al., Finite element analysis of auxetic obstacle deformation and fluid flow in a channel, J. Non-Cryst. Solids 355 (2009) 1387–1392.

[16] T. Strek, H. Jopek, Effective mechanical properties of concentric cylindrical composites with auxetic phase, Phys. Status Solidi B (2012) 1–7, http://dx.doi.org/10.1002/pssb.201084218.

[17] T. Strek, H. Jopek, B.T. Maruszewski, et al., Computational analysis of sandwich-structured composites with an auxetic phase, Phys. Status Solidi B 251 (2) (2014) 354–366.

[18] T. Strek, H. Jopek, M. Nienartowicz, Dynamic response of sandwich panels with auxetic cores, Phys. Status Solidi B (2015) 1–11, http://dx.doi.org/10.1002/pssb.201552024.

[19] Gabriele Imbalzano, Phuong Tran, Tuan D. Ngo, et al., Three dimensional modelling of auxetic sandwich panels for localised impact resistance, J. Sandw. Struct. Mater. (2015), http://dx.doi.org/10.1177/1099636215618539.

[20] N.T. Duong, N.D. Duc, Evaluation of elastic properties and thermal expansion coefficient of composites reinforced by randomly distributed spherical particles with negative Poisson's ratios, Compos. Struct. 153 (2016) 569–577.

[21] H. Jopek, T. Strek, Thermal and structural dependence of auxetic properties of composite materials, Phys. Status Solidi B 252 (7) (2015) 1551–1558.

[22] N.D. Duc, P.H. Cong, Nonlinear dynamic response and vibration of sandwich composite plates with negative Poisson's ratio in auxetic honeycombs, J. Sandw. Struct. Mater. (2016), http://doi.org/10.1177/1099636216674729.

[23] N.D. Duc, Nonlinear Static and Dynamic Stability of Functionally Graded Plates and Shells, Vietnam National University Press, Hanoi, 2014.

[24] N.D. Duc, Homayoun Hadavinia, P.V. Thu, T.Q. Quan, Vibration and nonlinear dynamic response of imperfect three-phase polymer nanocomposite panel resting on elastic foundations under hydrodynamic loads, Compos. Struct. 131 (2015) 229–237.

[25] N.D. Duc, T.Q. Quan, Nonlinear response of imperfect eccentrically stiffened FGM cylindrical panels on elastic foundation subjected to mechanical loads, Eur. J. Mech. A, Solids 46 (2014) 60–71.

[26] N.D. Duc, H.V. Tung, Nonlinear response of pressure-loaded functionally graded cylindrical panels with temperature effects, Compos. Struct. 92 (7) (2010) 1664–1672.

[27] N.D. Duc, Nonlinear dynamic response of imperfect eccentrically stiffened FGM double curved shallow shells on elastic foundation, Compos. Struct. 2013 (102) (2013) 306–314.

[28] K.T. Tan, H.H. Huang, C.T. Sun, Blast-wave impact mitigation using negative effective mass density concept of elastic metamaterials, Int. J. Impact Eng. 64 (2014) 20–29.

[29] S.D. Adhikary, L.R. Chandra, A. Christian, et al., Influence of cylindrical charge orientation on the blast response of high strength concrete panels, Eng. Struct. (2016), http://dx.doi.org/10.1016/j.engstruct.2016.04.035.

[30] C. Zhai, L. Chen, H. Xiang, et al., Experimental and numerical investigation into RC beams subjected to blast after exposure to fire, Int. J. Impact Eng. 97 (2016) 29–45.

[31] S. Yao, D. Zhang, X. Chen, et al., Experimental and numerical study on the dynamic response of RC slabs under blast loading, Eng. Fail. Anal. 66 (2016) 120–129.

[32] N. Lam, P. Mendis, N. Tuan, Response spectrum solutions for blast loading, Electr. J. Struct. Eng. 4 (2004) 28–44.

[33] G. Imbalzano, P. Tran, T.D. Ngo, et al., A numerical study of auxetic composite panels under blast loadings, Compos. Struct. 135 (2016) 339–352.

[34] C. Ding, T. Ngo, P. Mendis, et al., Dynamic response of double skin façades under blast loads, Eng. Struct. 123 (2016) 155–165.

[35] N.D. Duc, N.D. Tuan, T. Phuong, T.Q. Quan, Nonlinear dynamic response and vibration of imperfect shear deformable functionally graded plates subjected to blast and thermal loads, Mech. Adv. Mat. Struct. 24 (4) (2016) 318–329.